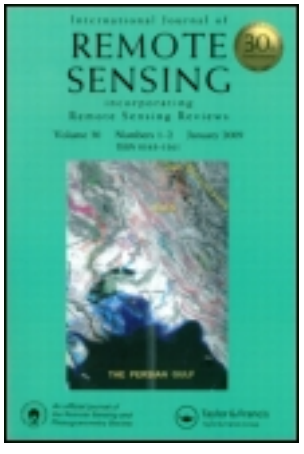

International Journal of Remote Sensing

Publication details, including instructions for authors and subscription information:
http://www.tandfonline.com/loi/tres20

Radiometric normalization for change detection in peatlands: a modified temporal invariant cluster approach

Jerome O'Connell [a], John Connolly [b], Eric F. Vermote [c] & Nicholas M. Holden [a]

[a] School of Biosystems Engineering, Agriculture and Food Science Centre, University College Dublin, Belfield, Dublin, 4, Ireland

[b] Department of Geography, University College Cork, Cork, Ireland

[c] Terrestrial Information Systems Branch/Code 614.5, NASA-Goddard Space Flight Center, Greenbelt, MD, 20771, USA

Published online: 18 Jan 2013.

To cite this article: Jerome O'Connell , John Connolly , Eric F. Vermote & Nicholas M. Holden (2013) Radiometric normalization for change detection in peatlands: a modified temporal invariant cluster approach, International Journal of Remote Sensing, 34:8, 2905-2924, DOI: 10.1080/01431161.2012.752886

To link to this article: http://dx.doi.org/10.1080/01431161.2012.752886

International Journal of Remote Sensing, 2013
Vol. 34, No. 8, 2905–2924, http://dx.doi.org/10.1080/01431161.2012.752886

Taylor & Francis
Taylor & Francis Group

Radiometric normalization for change detection in peatlands: a modified temporal invariant cluster approach

Jerome O'Connell[a]*, John Connolly[b†], Eric F. Vermote[c], and Nicholas M. Holden[a]

[a]*School of Biosystems Engineering, Agriculture and Food Science Centre, University College Dublin, Belfield, Dublin 4, Ireland;* [b]*Department of Geography, University College Cork, Cork, Ireland;* [c]*Terrestrial Information Systems Branch/Code 614.5, NASA-Goddard Space Flight Center, Greenbelt, MD 20771, USA*

(*Received 14 May 2011; accepted 17 July 2012*)

Radiometric normalization is a vital stage in any change detection study due to the complex interactions of radiance and irradiance between the Earth's surface and atmosphere. Compensation for variables such as sun's angle, surface profile, atmospheric conditions, and sensor calibration coefficients are essential in achieving a radiometrically stable data base of multi-temporal, multi-spectral imagery for a change detection study. In this study, five Landsat Enhanced Thematic Mapper Plus (ETM+) images taken over the east coast of Ireland in 2001 were geometrically corrected and topographically normalized for further processing and analysis. Assessment of various vegetation indices showed that the enhanced vegetation index 2 (EVI2) gave the highest accuracy in identifying the various vegetation types and habitats in the Wicklow Mountains National Park. The initial analysis of radiometric normalization with temporal invariant clusters (TICs) gave poor results due to the spectral heterogeneity of urban pixels within each image. A revised TIC subset normalized method was developed using regional growth parameters in urban environments to limit the spatial and spectral extent of pixels used in the TIC scene normalization process. Correlation analysis between the TIC-subset-normalized ETM+ data and Landsat Ecosystem Disturbance Adaptive Processing System (LEDAPS) absolute corrected data produced coefficient of determination (R^2) values between 0.88 and 0.98. Such results demonstrated the robustness of the TIC subset normalization procedure when correcting for atmospheric variability between images while maintaining spectral integrity. Statistical analysis on master slave and TIC-subset-normalized slave data using cumulative distribution curves derived from image histograms showed an 86.93% reduction in the maximum difference between master and slave data due to the TIC subset normalization process. This procedure of radiometric normalization is suitable in landscapes with a low density of spectrally stable targets.

1. Introduction

Peatlands contain approximately one-third of the global terrestrial soil carbon stock (547×10^9 tonnes) on only 4–6% of the terrestrial land area (Yu et al. 2010). Living biomass is fundamental to the carbon (C) cycle in peatlands as it is the main source of C input to peat

*Corresponding author. Present address: School of Biology, Faculty of Biological Sciences, University of Leeds, UK. Email: J.O'Connell@leeds.ac.uk.
†Present address: Department of Physical Geography & Ecosystem Science, Lund University, Sölvegatan 12, SE-223 62 Lund, Sweden.

soil. Extensive anthropogenic disturbance, such as drainage of unspoiled peatland habitats, can have negative impacts on C sequestration rates, and in extreme cases, can convert such habitats from net sinks to a net sources of C emissions through oxidization of C stock (Tallis 1998; Bragg and Tallis 2001). Soil organic carbon (SOC) can be regarded as a biosphere sink under the Kyoto Protocol/Marrakech Accords (Articles 3.3 and 3.4) (Kyoto Protocol 1997). In Ireland, approximately 20% of the land area is covered by peatlands (Connolly, Holden, and Ward 2006). This accounts for between 53% (1071×10^6 tonnes C) and 62% (1503×10^6 tonnes C) of the country's national soil carbon stock (Tomlinson 2005; Eaton et al. 2008). Ireland has a commitment to reducing net carbon emissions by 20%, currently specified at 66.216×10^6 tonnes yearly, averaged over the period of 2008–2012 (Brennan and Curtin 2008). Given that the Irish peatland resource is subject to significant anthropogenic disturbance (Tallis 1998), quantification of the effect of disturbance on the peatland carbon pool will be an important part of climate change management policy in the future.

Remote-sensing technology can be used to monitor, assess, and quantify changes in peatland vegetation over time. It is particularly suitable for this task due to the remoteness and extent of many peatland areas (Ozesmi and Bauer 2002; Connolly et al. 2011). Significant variation in spectral signature can be indicative of some form of anthropogenic disturbance (O Connell 2012) in peatland vegetation. Remote sensing can potentially provide spatially extensive, temporally frequent quantification of vegetation disturbance on peatland.

Remote-sensing technology can be used to monitor, assess, and quantify changes in peatland vegetation over time. (Ozesmi and Bauer 2002; Connolly et al. 2011). Significant variation in spectral signature can be indicative of some form of anthropogenic disturbance (O Connell 2012) in peatland vegetation. Remote sensing can potentially provide spatially extensive, temporally frequent quantification of vegetation disturbance on peatland. Radiometric normalization is an essential part of any change detection study using remotely sensed imagery (Lillesand, Kiefer, and Chipman 2004). Radiance measured by satellite sensors is a result of a complex interaction between target surface condition, sun's angle, Earth–Sun distance, sensor calibration, atmospheric properties, and Sun–target–sensor geometry (McGovern et al. 2002). These radiometric properties vary with time, therefore change detection studies must quantify and account for these differences in order to produce accurate change detection measurements. There are two radiometric correction options available: absolute and relative.

Absolute correction is an image-specific procedure that estimates at-surface reflectance for target objects by compensating for atmospheric absorption by gases and scattering by aerosols and water vapour (Vicente-Serrano, Perez-Cabello, and Lasanta 2008). Radiative transfer models are used to quantify atmospheric and electromagnetic properties at the time of image acquisition. *In situ* atmospheric information is usually required to apply these methods. However, some approaches, such as 'Second Simulation of the Satellite Signal in the Solar Spectrum' (6s) (Vermote et al. 1997), can use pre-defined atmospheric models and reduce the need for radiosonde data. While aerosol optical properties are an important constituent in atmospheric correction, some authors have shown that it can be constrained to a few modes that have shown acceptable performance over land (Levy, Remer, and Dubovik 2007).

Absolute correction can have poor radiometric consistency between images when compared to some relative normalization procedures (Schroeder et al. 2006) and a lack of *in situ* atmospheric data such as aerosol optical depth can produce uncertain results (Song et al. 2001; Schroeder et al. 2006). This uncertainty can lead to problems of low accuracy in change detection studies.

Relative normalization corrects images to the same radiometric scale as a pre-defined master or reference image, thereby eliminating the need for radiosonde data by assuming a linear relationship between images based on invariant or radiometrically stable targets (Song et al. 2001). This procedure reduces the radiometric variability between images, and is often preferred to absolute correction for change detection studies (Janzen, Fredeen, and Wheate 2006; Vicente-Serrano, Perez-Cabello, and Lasanta 2008). Schroeder et al. (2006) examined a variety of different absolute and relative correction methods on a multi-temporal data base of Landsat data in the forests of Western Oregon, USA. They found that absolute normalization (i.e. at surface reflectance data normalized to a master image) using invariant pixels selected by multivariate alteration detection (MAD) and manually selected pseudo-invariant features (PIF) produced the best results. Many of the methods used in relative normalization can be region or habitat specific (Lillesand, Kiefer, and Chipman 2004) and the selection of invariant targets is important (Chen, Vierling, and Deering 2005; Paolini et al. 2006) as they need to be radiometrically stable in relation to the temporal scale of the imagery in order to allow vegetation change to be detected accurately. Invariant targets typically consist of man-made structures (e.g. large buildings, motorways, or car parks), deep waterbodies (e.g. lakes or reservoirs), and vegetation with little phenological activity (e.g. mature conifer forest). Peatlands typically have few such targets, so radiometric normalization has to be undertaken at a scene scale large enough to encompass features peripheral to the area of interest. Du, Teillet, and Cihlar (2002) used a fully automated principal component analysis (PCA) with pre-defined thresholds. Hajj et al. (2008) settled on a 7% standard deviation threshold to select invariant pixels from a multi-band difference image (MDI). The Irish landscape also lacks large-scale spectrally stable urban environments due to the low population density (60 persons per km^2 in 2006), and the ribbon-like development of many towns and villages (CSO 2006). McGovern et al. (2002) indicated the difficulty of selecting urban invariant targets in the midlands of Ireland due to the scale of the urban environments in relation the resolution of the satellite imagery. Targets can be selected manually (Eckhardt, Verdin, and Lyford 1990), or automatically using statistical analysis (Hajj et al. 2008). McGovern et al. (2002) used a digital number (DN) threshold-based method for extraction of urban pixels in a Landsat Thematic Mapper (TM) image of the midlands of Ireland where few consistent targets could be manually identified.

To achieve an accurate radiometric normalization of satellite imagery in Ireland requires a spatially sensitive extraction procedure for invariant urban and deep-water environments. Chen, Vierling, and Deering (2005) proposed the use of point density maps in the selection of temporal invariant clusters (TICs) in the boreal forests of Krasnoyarsk Kay, Russia. Vegetation index (VI) images from two Landsat Enhanced Thematic Mapper Plus (ETM+) scenes were plotted on a 2D scatter plot that was used to create a point density map to identify clusters of pixels of similar values. The linear regression of the TICs was used to create a no-change axis, the slope and intercept of which were then used for relative radiometric normalization of slave to master images. For radiometric normalization of peatland scenes in Ireland, the approach of Chen, Vierling, and Deering (2005) (referred to hereafter as TIC scene normalization) has several advantages: only two invariant clusters need to be identified for the regression; the density of pixels within the TICs is not critical to the overall accuracy of the process; a large spatial expanse of invariant objects is not necessary in every image; and the TIC scene normalization can be applied to uncorrected VI images thus reducing data storage requirements and processing time when dealing with a large data base of multi-spectral imagery (Chen, Vierling, and Deering 2005). For these reasons, the TIC approach was adopted for this study.

The specific objective of this article is to present and assess a radiometric normalization procedure to correct a multi-spectral, multi-temporal data base of satellite imagery for Ireland that can be semi-automated and is suitable for vegetation change detection in the peatland environment. There are vast tracts of peatland around the northern polar arc that have similar characteristics of limited atmospheric data for absolute correction and few radiometrically invariant features suited to standard relative normalization procedures. Therefore, the procedure developed for peatland in Ireland will have a wide global relevance.

2. Method

2.1. Study site

Validation of the radiometric normalization procedure was conducted for images of the Wicklow Mountains National Park, which contains approximately 130 km^2 of Montane blanket bog on the east coast of Ireland (53° 09′ N, 6° 18′ W) (Figure 1). Annual rainfall is between 1300 and 2400 mm, with low evapotranspiration for most of the year due to high altitude and low temperatures (Tallis 1998; Connolly et al. 2011). Much of the Wicklow Mountains is protected by Irish and EU habitat directives; however, anthropogenic disturbance of peatland vegetation is prominent throughout the area. Peat harvesting, drainage and land reclamation, afforestation, burning, and over–grazing – all threaten the ecology of this environment, and may have implications for the current and future soil organic carbon stock.

2.2. Data

In 2001, Landsat ETM+ was able to capture five cloud-free images over the east coast of Ireland, which were suitable for this study (Table 1). The data were acquired from the US Geological Surveys Global Visualization Viewer with standard terrain correction (Level 1T) applied (USGS 2010). A detailed habitat map of the Wicklow Mountains was obtained from the National Parks and Wildlife Service (NPWS 2007) to assist with the interpretation of spectral data and vegetation indices (Figure 1). This map was derived from 5 m resolution Quickbird and 20 m resolution Système Pour l'Observation de la Terre (SPOT) multi-spectral imagery acquired in the summer of 2006, with the classification scheme based on Fossitt (2000). A Landsat TM image also acquired in the summer of 2006 (Table 1) was used in conjunction with habitat map in the analysis of vegetation indices. Shadowing effects had to be taken into account due to the latitude (53°N) of the study area and low sun elevation (<25°) in the period of November to March. A 20 m digital elevation model (DEM) was obtained from the Irish Environmental Protection Agency (EPA) to provide necessary data on the relief in the study area.

2.3. Data pre-processing

Several pre-processing procedures were applied to the imagery throughout the normalization process (Figure 2). These are outlined in the following sections.

2.3.1. Georectification

First, all images were geo-registered to a pre-defined master image using the AutoSync tool in Erdas Imagine 9.3. The master image (image 4 in Table 1) was selected because it was

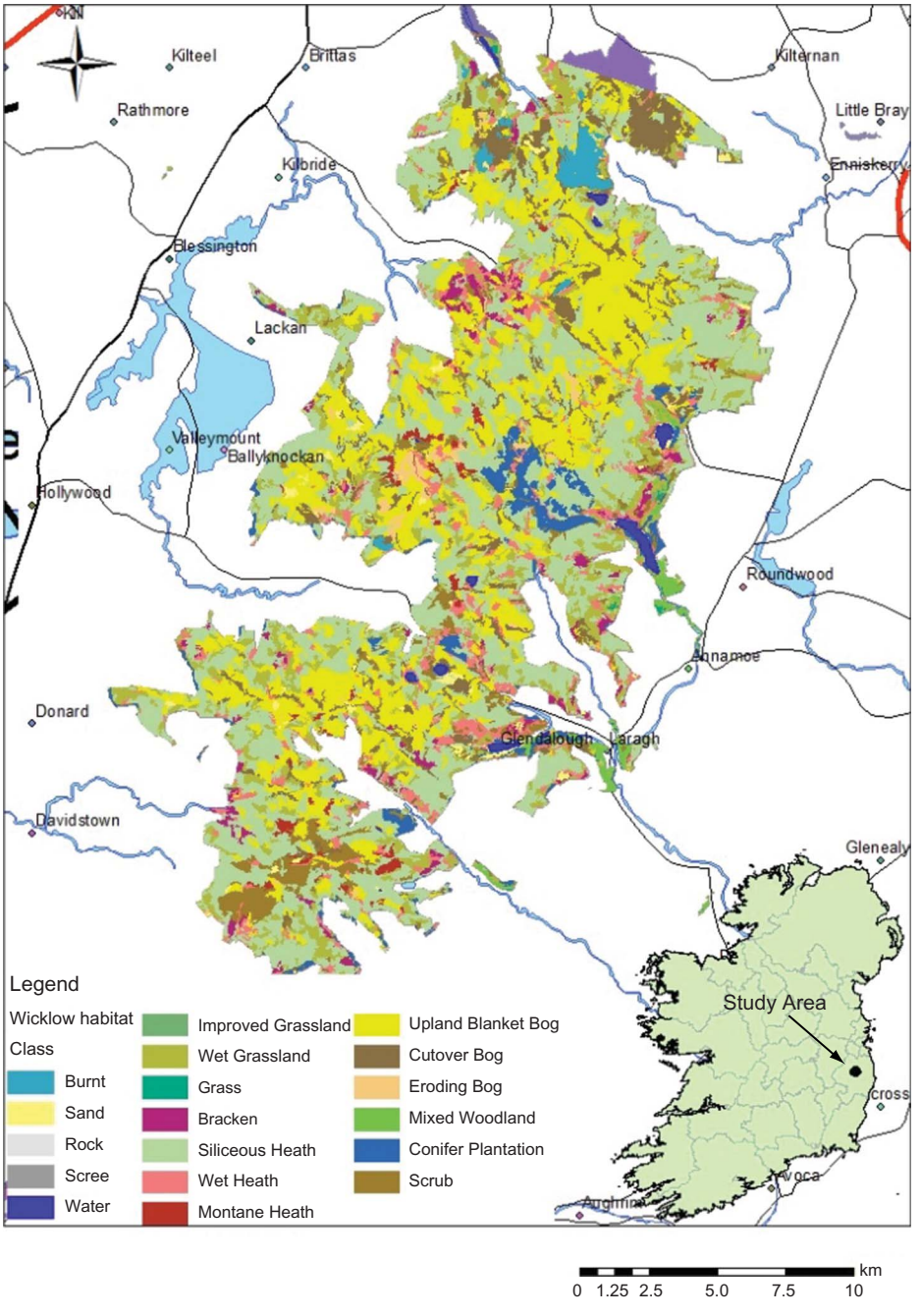

Figure 1. Map of The Wicklow Mountains National Park with Quickbird-/SPOT-derived habitat map (NPWS 2007).

in the middle of the temporal sequence and had a good radiometric quality. A projective transform model was used in conjunction with the 20 m DEM and a root mean squared error (RMSE) threshold of 0.3 with cubic convolution resampling to achieve sub-pixel-level accuracy $\leq$10% as required for change detection studies (Coppin et al. 2004).

Table 1. Metadata for Landsat ETM+ and TM images used in the TIC subset normalization process.

Image no.	Platform	Date	Path	Row	Solar elevation (°)	Solar azimuth (°)	Solar distance (au)
1	ETM+	17 February 2001	206	23	22.388	156.811	0.98814
2	ETM+	8 May 2001	206	23	51.527	152.323	1.00928
3	ETM+	24 May 2001	206	23	54.966	150.268	1.01267
4	**ETM+**	**28 August 2001**	**206**	**23**	**43.840**	**153.414**	**1.01015***
5	ETM+	31 October 2001	206	23	21.504	164.620	0.99279
6	ETM+	24 February 2001	207	23	24.888	156.340	0.98966
7	ETM+	2 July 2001	207	23	56.415	145.988	1.01670
8	TM	17 July 2006	206	23	54.891	147.834	1.01635

Notes: Image 4 (highlighted in bold) was selected as the pre-defined master image for radiometric normalization. Image 8 was used in the analysis of vegetation indices. Solar distance, expressed in astronomical units (au), refers to the mean sun to earth distance (149, 597, 870, 700 m).

2.4. Vegetation index

VIs are an established method of monitoring vegetation from space (Rondeaux, Steven, and Baret 1996). Vegetation indices can also be highly correlated to vegetation health, abundance, and vigour, as well as physical measurements such as leaf area index (LAI) and gross primary production (GPP) (Huete et al. 1997; Jiang et al. 2008). In this study it was deemed necessary to assess various VIs in detecting the various vegetation communities of the Wicklow Mountains. Four different indices were tested by calculating the VI for a Landsat TM image recorded over the east coast of Ireland on 17 July 2006. This image was acquired within 25 days of an NPWS 2006 habitat map (NPWS 2007), therefore the variation in vegetation and habitat distribution was minimal. Band 5 from Landsat TM was used for the shortwave infrared (SWIR) reflectance necessary for the normalized difference moisture index (NDMI). The VIs tested were as follows.

- Normalized difference vegetation index (NDVI):

$$\mathrm{NDVI} = \frac{(\mathrm{NIR}) - \mathrm{R}}{(\mathrm{NIR}) + \mathrm{R}} \text{ (Sellers 1985).}$$

- Normalized difference moisture index (NDMI):

$$\mathrm{NDMI} = \frac{(\mathrm{NIR}) - (\mathrm{SWIR})}{(\mathrm{NIR}) + (\mathrm{SWIR})} \text{ (Wilson and Sader 2002).}$$

- Modified soil adjusted vegetation index (MSAVI):

$$\mathrm{MSAVI} = \frac{2 \times (\mathrm{NIR}) + 1 - \sqrt{(2 \times (\mathrm{NIR}) + 1) - 8\,((\mathrm{NIR}) - (\mathrm{R}))}}{2} \text{ (Qi et al. 1994).}$$

- Enhanced vegetation index 2 (EVI2):

$$\mathrm{EVI2} = 2.5\frac{(\mathrm{NIR}) - \mathrm{R}}{(\mathrm{NIR}) + 2.4\mathrm{R} + 1} \text{ (Jiang et al. 2008),}$$

where NIR refers to near-infrared reflectance and R refers to red reflectance.

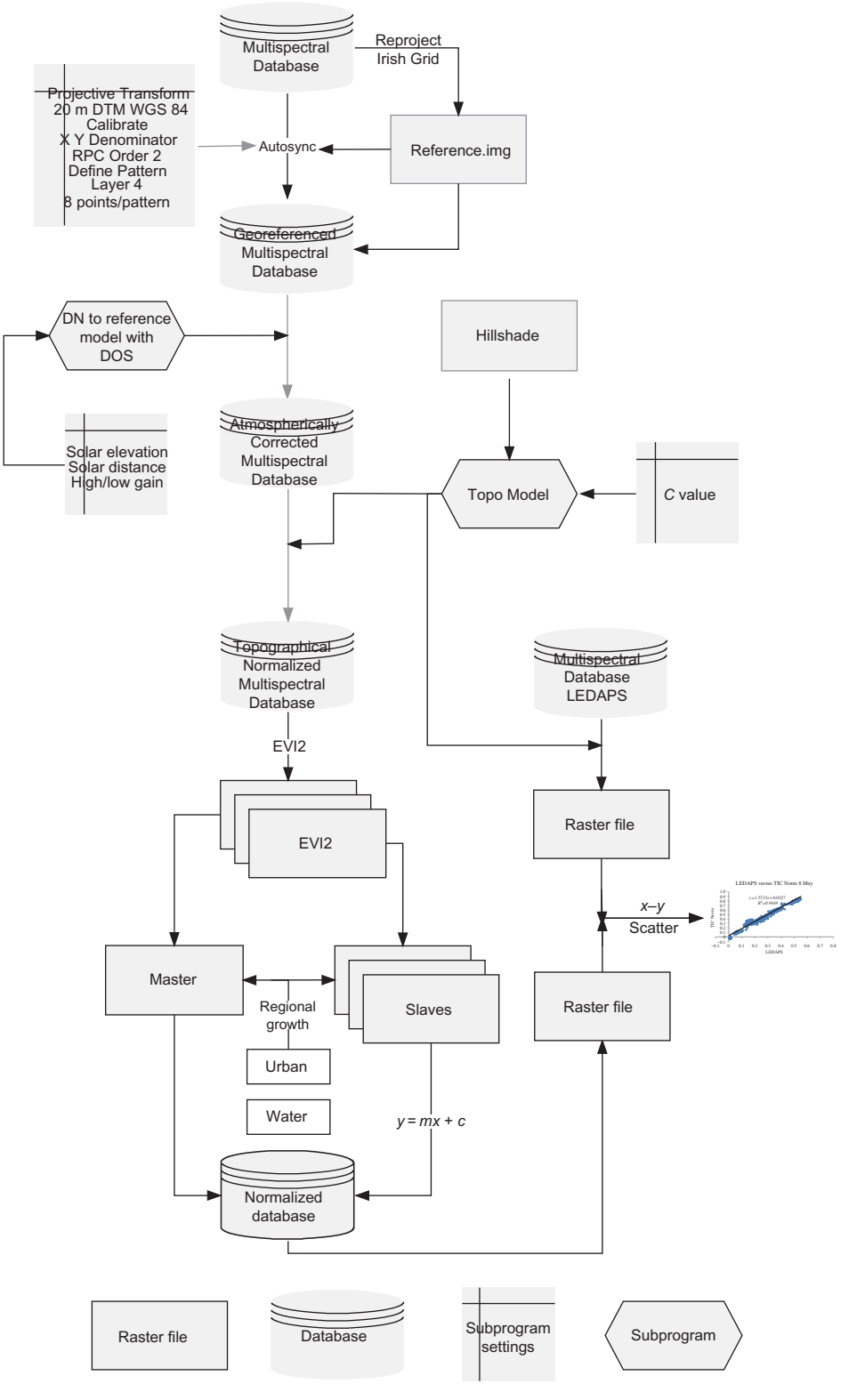

Figure 2. Conceptual model of TIC subset normalization and validation process.

Each index was assessed based on its ability to depict the various vegetation and habitat types of the Wicklow Mountains National Park using the NPWS 2006 habitat map as a baseline data set. The index that best encapsulated the vegetation of this area would then be selected for further analysis in the area of radiometric normalization. Stratified random sample points were taken within the boundaries of Wicklow Mountains National Park (Figure 1, note that individual sampling points are not shown due to the map scale) based on the NPWS 2006 habitat map. The criterion for the sampling procedure was a minimum of 40 sample points per habitat class, thereby ensuring good coverage of spectral data across all vegetation types within the study area. The sample points were then used to interpolate spectral data from the various VIs to assess the ability of each index to depict the various vegetation communities within the Wicklow Mountains National Park.

2.5. Radiometric normalization

Chen, Vierling, and Deering (2005) outlined the procedure for performing TIC analysis on complete Landsat images. The procedure involved the use of point-density plots and the identification of two or more invariant clusters in the delineation of a regression line. Initially it was found that TIC analysis of complete images (i.e. TIC scene normalization) was not suitable in our study site due to the diversity of spectral signatures within the image and the lack of spatially extensive invariant targets making it difficult to identify TIC centres resulting in poor regression fits. A preliminary evaluation also showed that vegetation and soil pixels were contaminating the urban clusters due to the dispersed nature of Irish settlements. Instead, homogeneous areas of urban and water pixels were manually identified in each image using density slices, and plotted to create TICs with reduced spectral diversity. The process (Figure 2) began with all imagery being converted from DN scale to at-sensor radiance (units: W m^{-2} sr^{-1}), using the L_{MAX} L_{MIN} equations in the Landsat 7 Users Handbook (NASA 1998). These data were then converted to top-of-atmosphere reflectance using Equation (1) to reduce radiometric variability between images (Richards and Jia 2006):

$$\rho_{ASR} = \frac{(\pi L_{sat})}{E_o \cos\phi}, \tag{1}$$

where ρ_{ASR} is unitless top-of-atmosphere reflectance, L_{sat} is pixel radiance, E_o is exo-atmospheric solar constant (W m^{-2} sr^{-1}), and ϕ is solar zenith angle. Dark object subtraction (DOS) was then implemented to all imagery in the data base to reduce radiometric variability between images due to atmospheric scattering (Chen, Vierling, and Deering 2005). DOS was applied by calculating the mean of the lowest 5% of pixel values in the image histogram.

The location of the urban and water pixels for the TIC subset normalization method was established by density slicing master and slave images. A regional growth function (in Erdas Imagine 9.3) was used to create area of interest (AOI) files of homogeneous pixels from each region. The size and shape of the AOI file was limited by area and spectral distance, typically 200 ha and $\pm$ 0.04 EVI2. Once the AOI files were delineated, pixels from the master and slave images were extracted and plotted on an x–y scatter plot (Figure 2). Data were then transferred to ArcMap (ESRI 2010) and the centres for both clusters were established with the mean centre function in spatial analyst method. By using this method of delineating the cluster centres, we avoided the subjectivity of the manual selection proposed by Chen, Vierling, and Deering (2005). The issue of outliers in the data

due to mis-registration or cloud cover was eliminated by applying a threshold function to the data, e.g. 'if $x - y > 0.25$' then delete the point.

2.5.1. Radiometric validation

Radiometric variation between images can occur due to changes in sensor response and calibration, illumination angles, atmospheric effects, reflectance anisotropy, and topography (Paolini et al. 2006). These variables can often be affected by the temporal distance between the master and slave images in a normalized data base, therefore it is important to quantify their effect on normalization accuracy. Correlation analysis between the TIC relative normalization and at-surface absolute correction was used to assess the influence of temporal distance between master and slave images in the TIC subset normalization method (Figure 2). Absolute correction was achieved using the Landsat Ecosystem Disturbance Adaptive Processing System (LEDAPS) (Masek et al. 2006). This software achieves at-surface reflectance for full Landsat ETM +/TM scenes by applying the MODAPS software architecture (Justice et al. 2002) with 6s radiative transfer code (Vermote et al. 1997). The Erdas Imagine AutoSync tool was then used to register the LEDAPS data to the corresponding TIC subset normalization images, ensuring sub-pixel-level spatial correlation between the two data sets.

2.6. Topographical normalization

The combination of low sun angle and rugged terrain can lead to irregularities in sun's illumination between north- and south-facing slopes. This means that uniform vegetation may display radiance variations due to illumination effects caused by slope, aspect, and time of image acquisition. Change detection studies require that this issue be resolved (Civco 1989; Riaño al. 2003; Gao and Zhang 2009). The correction procedure outlined by Nichol, Hang, and Sing (2006) was applied to the data in this study to reduce the effect of shadowing on north-facing slopes in the 17 February and 31 October images (Table 1).

3. Results and discussion

3.1. Vegetation indices

In this study the specific dynamics of VIs for peatland habitats was investigated. The scatter plot of EVI2 versus NDVI (Figure 3(*a*)) for the various habitats in the Wicklow Mountains shows a curvilinear relationship, with NDVI producing higher index values throughout. As the graph approaches 1.0 in both axes, the trajectory of the NDVI data tends to flatten out. NDVI is prone to 'saturation' in highly vegetated habitats (Rondeaux, Steven, and Baret 1996; Teillet, Staenz, and William 1997) due to sensitivity to the 'red shoulder of vegetation' (i.e. red–NIR). This is illustrated by the relatively high values for Upland Blanket bog when compared to EVI2 (Figure 3(*a*)). In summer this habitat tends to have a low NIR-to-red ratio, giving a high NDVI value. Soil contamination of NDVI can also be problematic (Huete et al. 1997), with pixels classified as 'Burnt' (Figure 3(*a*)) having much higher NDVI than EVI2 values. EVI2 overcomes the issue of soil background contamination by placing additional weighting on red reflectance data (Rocha and Shaver 2009).

In previous studies; NDMI has shown sensitivity to leaf structure, moisture content, and vegetation disturbance (Jin and Sader 2005). The range of NDMI for the Wicklow

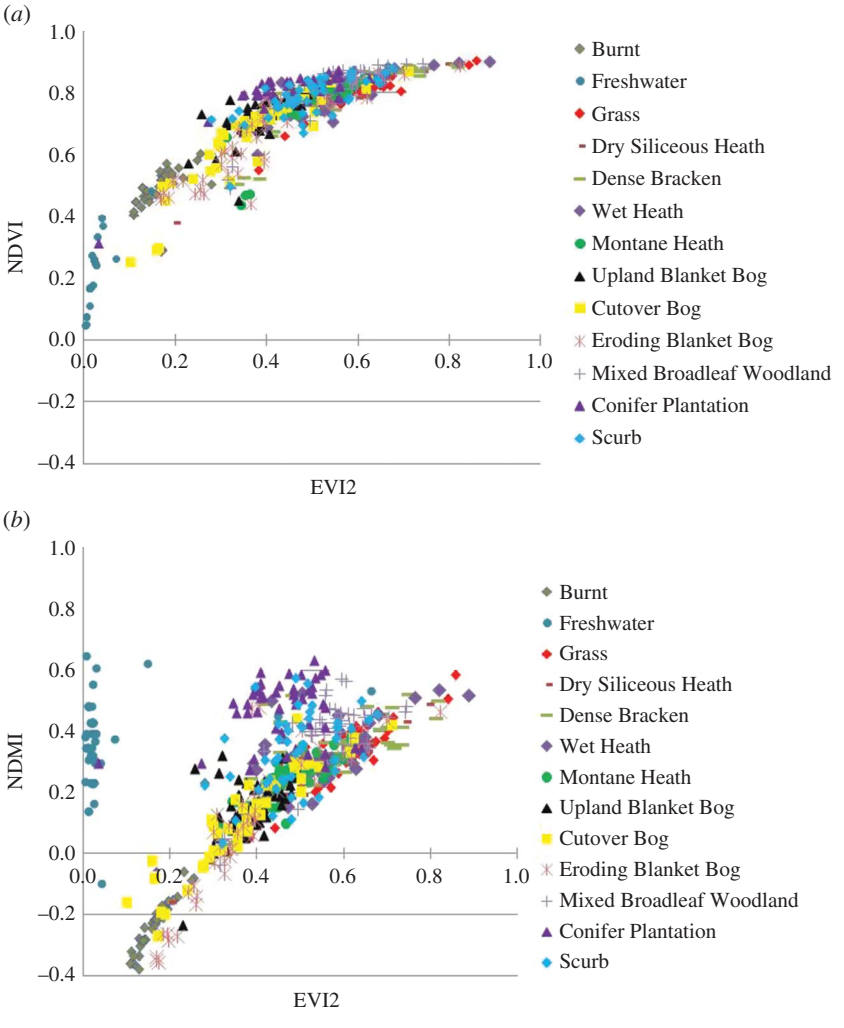

Figure 3. Scatter plots of (*a*) EVI2 versus NDVI and (*b*) EVI2 versus NDMI using stratified random samples from a Landsat TM image taken on 17 July 2006, over the Wicklow Mountains.

Mountains was much smaller than for all other indices (Figure 3(*b*)), with 'Burnt' vegetation producing the lowest value (–0.38) and 'Freshwater'/'Conifer Plantation' producing the highest (0.6). The correlation between EVI2 and NDMI was generally high except for 'Freshwater' and 'Conifer Plantation'. The inclusion of SWIR data in the NDMI index means it is especially sensitive to moisture. The structure of the EVI2 and MSAVI equations puts emphases on NIR reflectance (Rocha and Shaver 2009) and, despite variations in scale, both VIs show correlation to NIR, in both frequency and profile (Figure 4). The low spectral resolution of NDVI is illustrated by poor data dispersion across the VI range as well as the sudden drop in frequency on approaching 1.0, indicating index saturation (Figure 4). NDMI depicts high pixel frequency and, as a result, has relatively low spectral resolution with most pixels located in the 0.56–0.78 range.

Overall, the best VI for this study was selected based on its ability to detect the various vegetation communities within the Wicklow Mountains National Park. Previous

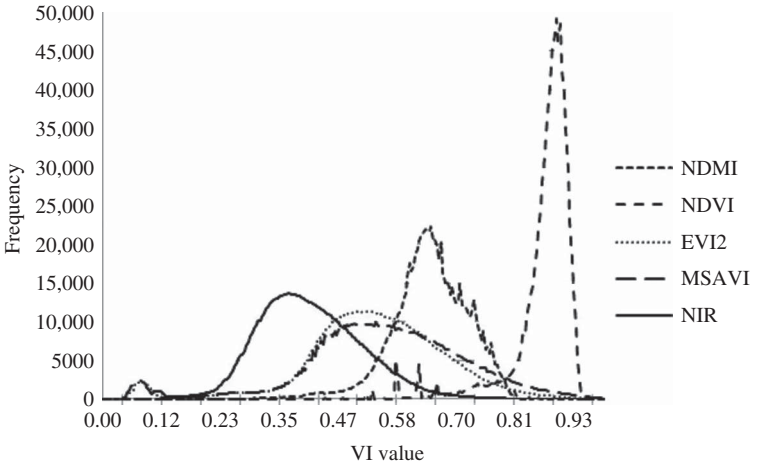

Figure 4. Image histograms of NIR and four vegetation indices derived from a Landsat TM image taken on 17 July 2006 over the Wicklow Mountains.

studies have shown that peatland habitats exhibit unique trends in relation to VI dynamics (McMorrow et al. 2004; Dabrowska-Zielinska et al. 2009; Hassan and Charles 2010). In this study NDVI produced the greatest index values throughout; however the saturation of the index in summer months, as well as effects of soil and atmospheric contamination, meant the index was unsuitable. NDMI, while showing good divergence between habitats, was judged to be erratic and patterns expected to be related to moisture content were not obvious, therefore NDMI was also deemed unsuitable. EVI2 and MSAVI worked well for the upland blanket bog habitat as the chlorophyll content of much of the vegetation was relatively low for much of the year. Indices that rely on high absorption in the red part of the electromagnetic spectrum (e.g. NDVI) will, as a result, have a low dynamic range of index values. NIR reflectance was generally high in these peatlands, mainly due to the variability in leaf structure within the various vegetation types. As a result, both EVI2 and MSAVI have showed a good dynamic range across most vegetation types. EVI2 has shown high correlation with LAI (Huete et al. 2002; Jiang et al. 2008; Rocha and Shaver 2009), which is an important parameter in the context of this study. It is for this reason that EVI2 was chosen over MSAVI as the preferred VI for further application to peatlands in Ireland.

3.2. Radiometric normalization

In this study, a new subset method of TIC scene normalization was developed and validated against the original method as well as absolute corrected LEDAPS data. Figure 5(*a*) shows the density plot for TIC subset normalization with the mean centre points for the urban and water clusters (marked red) in two Landsat ETM+ images recorded in February and July of 2001 (Table 1) over Limerick City (52° 39′ 45″ N, 8° 36′ 8″ W). Figure 5(*b*) shows the density plots for the original TIC scene normalization method, using the same images as Figure 5(*a*), but with all pixels included. The density plots were created by calculating the density of point features around each output raster cell (ESRI 2010). There is a slight change in location between the TIC scene normalization water cluster (Figure 5(*b*)) and the centre of the TIC subset normalization water cluster (Figure 5(*a*)). This is most likely due to the change in the population density of water pixels between the two plots, with the

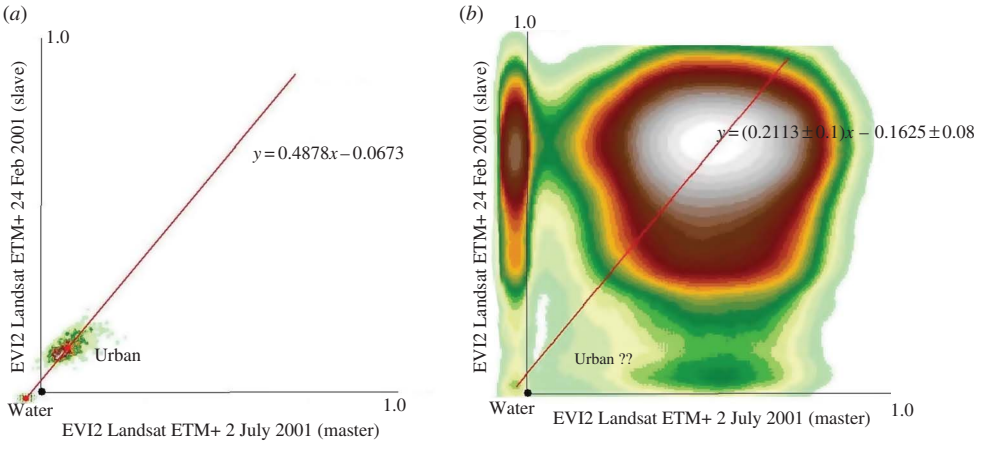

Figure 5. Density plots for two Landsat ETM+ images (2 July 2001 (master) and 24 February 2001 (slave)) over Limerick City with regression lines for TIC subset normalization: (*a*) TIC scene normalization, (*b*) and accompanying linear regression equations. Red dots show mean centres for urban and water for TIC subset normalization.

TIC scene normalization plot having a significantly larger group of water pixels present, with varying degrees of reflectance. In terms of the urban clusters, the mean centre function used in the TIC subset normalization method implies that its location is statistically and spectrally accurate, resulting in a true representation of the radiometric relationship between the master and slave images. The urban cluster for the TIC scene normalization plot (Figure 5(*b*)), however, is more difficult to identify due to the inclusion of all pixels in both images, resulting in a large population of heterogeneous data. This was reflected in the uncertainty in the regression equation.

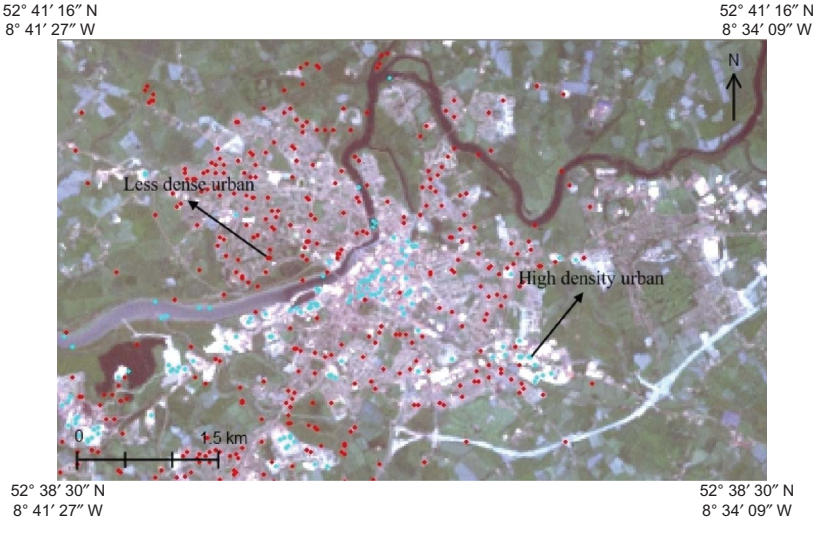

Figure 6. The variation between TIC scene normalization selected urban cluster pixels (red dots) and the TIC subset normalization selected urban cluster pixels (blue dots) in Limerick City using two Landsat ETM+ images acquired on 24 February (slave) and 2 July (master) 2001.

The effect of using the subset method of urban pixel selection compared to the TIC scene normalization revealed a clear variation in urban pixel selection (Figure 6). The TIC scene normalization method resulted in pixels that were spectrally variable, with the inclusion of vegetation, silted water, and bare soil (Figure 6), while the subset method produced good spatial and spectral correlation with areas of urban development that could be used as invariant targets in the correction process. The TIC scene normalization density plot (Figure 5(*b*)) is condensed in a large cloud of pixel values constituting much of the spectra of both images. Successful selection of TIC centres depends on such observation of the point density map and evaluation of the master and slave images as to confirm that the pixels located in the TIC centres are true invariant features (Chen, Vierling, and Deering 2005). In our study area, using the scene point density map (Figure 5(*b*)) to identify cluster centres was difficult because of the lack of spatially extensive invariant targets such as urban environments or large waterbodies. Thus for non-expert TIC users, delineating the regression line from the TIC scene normalization plot is subjective and prone to uncertainty. The degree of uncertainty in the regression equation [$y = (0.2113 \pm 0.1)x - 0.1625 \pm 0.08$] would lead to potentially large errors in the radiometric normalization process. The homogeneity of the clusters, coupled with the systematic approach to calculating cluster centres, means that the TIC subset normalized method developed in this study is superior to the TIC scene normalization when dealing with the landscape of Ireland.

3.2.1. Validation

Validation of any radiometric normalization procedure is essential for ensuring spectral accuracy and radiometric continuity throughout the data base. In this study, TIC normalized data were correlated to at-surface absolutely corrected LEDAPS data so as to quantify the deviation of the normalized data from its original state. Summary statistics were calculated on the five ETM+ images, with regard to the original EVI2 data (Orig in Table 2), TIC-subset-normalized EVI2 data (TIC in Table 2), and absolute corrected data (LEDAPS in Table 2). The mean EVI2 for the TIC normalized data stays within the range of 0.38–0.33 throughout all images, demonstrating the effect that the normalization process has on reducing the radiometric variability between the imagery. While no ground truth data were available as part of this study to verify that actually vegetation change had been unaffected by the TIC subset normalization process, work completed in conjunction with this study supports the robustness of this method (O Connell, Connolly, and Holden in review-b). The original data have a decreasing fluctuating mean trend, and show a far more dynamic profile when compared to the TIC-subset-normalized data set. The LEDAPS data exhibited a more heterogeneous trend in mean EVI2, with values ranging from 0.19 to 0.29. Standard deviation for the TIC-subset-normalized data set was relatively high, but consistent throughout the data set, signifying a high spectral dispersion across each image histogram, but with a low deviation due to the subset normalization process.

Linear regression analysis showed a high correlation between the TIC-subset-normalized and LEDAPS-corrected images across the five main land-use types within the study area (Figure 7). The general trend was an increased correlation with decreasing temporal distance from the master image (28 August). Pixels exhibited a greater spectral heterogeneity in the two winter images (Figures 7(*a*) and (*e*)), with a greater number of outliers, which resulted in lower coefficient of determination (R^2) values. However, the effect of increased temporal distance between master and slave images did not result in a considerable de-correlation of the TIC-subset-normalized data when compared to the LEDAPS images. The LEDAPS data produced lower EVI2 values throughout all images

Table 2. Summary statistics for five Landsat ETM+ images, for both TIC-subset-normalized and LEDAPS data.

	17 February			8 May			24 May			28 August		31 October		
	LEDAPS	TIC	Orig	LEDAPS	TIC	Orig	LEDAPS	TIC	Orig	LEDAPS	Orig	LEDAPS	TIC	Orig
Mean	0.233	0.361	0.257	0.192	0.338	0.290	0.217	0.336	0.304	0.266	0.379	0.292	0.334	0.298
St Error	0.001	0.002	0.001	0.001	0.002	0.002	0.001	0.002	0.002	0.001	0.002	0.001	0.002	0.002
Mediam	0.237	0.377	0.268	0.150	0.273	0.233	0.157	0.258	0.233	0.241	0.352	0.282	0.311	0.279
Mode	0.217	0.374	0.257	0.149	0.263	0.234	0.151	0.240	0.219	−0.004	−0.023	0.290	0.310	0.272
St Dev	0.092	0.153	0.107	0.104	0.192	0.168	0.141	0.210	0.189	0.134	0.191	0.140	0.205	0.169
Variance	0.008	0.023	0.011	0.011	0.037	0.028	0.202	0.044	0.036	0.018	0.036	0.020	0.042	0.029
Kurtosis	1.747	1.765	1.768	0.075	−0.010	−0.010	−0.132	−0.177	−0.177	−0.094	−0.031	0.548	0.309	0.309
Skewness	−0.405	−0.891	−0.871	0.915	0.724	0.724	0.931	0.770	0.770	0.215	0.012	0.373	0.285	0.285
Range	0.697	1.119	0.786	0.524	0.947	0.830	0.652	0.992	0.892	0.625	0.894	0.763	1.082	0.893
Minimum	−0.042	−0.100	−0.066	0.003	−0.027	−0.030	−0.020	−0.048	−0.041	−0.011	−0.038	−0.026	−0.132	−0.087
Maximum	0.655	1.019	0.719	0.526	0.920	0.800	0.632	0.945	0.851	0.614	0.856	0.737	0.950	0.807

Note: The abbreviation St Error indicates standard error; St Dev indicates the standard deviation; TIC refers to the TIC-subset-normalized data set; and Orig refers to the Original data set.

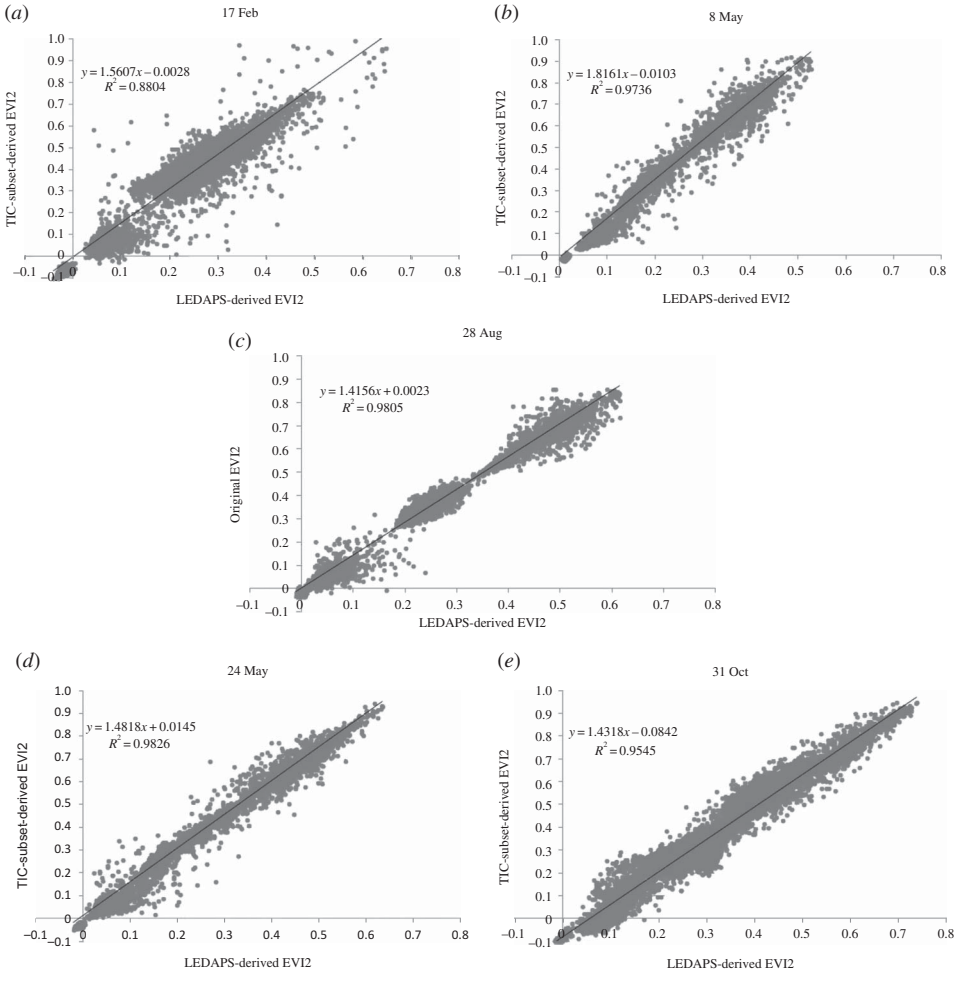

Figure 7. Scatter plots of absolute corrected (via LEDAPS) versus TIC subset normalization for the five ETM+ images over the Wicklow Mountains. (*a*) 17 February, (*b*) 8 May, (*c*) 28 August, (*d*) 24 May, and (*e*) 31 October. Original EVI2 indicates master data with no normalization applied.

in comparison to TIC subset normalization, illustrating the difference in atmospheric correction between simple DOS and the more complex absolute correction of the LEDAPS data.

The trend in overall mean EVI2 projects a gradual development in growth patterns for TIC-subset-normalized data base (Figure 8(*a*)). The original data set (i.e. no normalization) indicated a typical phenological distribution, with low values at the start and end of the growing season, and peak values around July and August. The normalized data set on the other hand, indicated a narrow range, with small variation throughout the growing season. The reduced range of the normalized images has a clear advantage for change detection analysis because the scale and threshold level of change will be significantly reduced, resulting in a more sensitive and accurate set of change detection results. The LEDAPS data showed a minimum value for early May with an increasing trend for the remainder of the season. This trend, despite not following the typical phenological pattern of a natural habitat (i.e. low winter followed by high summer growth), has been exhibited in other peatland sites in Ireland in terms of satellite-derived EVI2 data and ground-based LAI

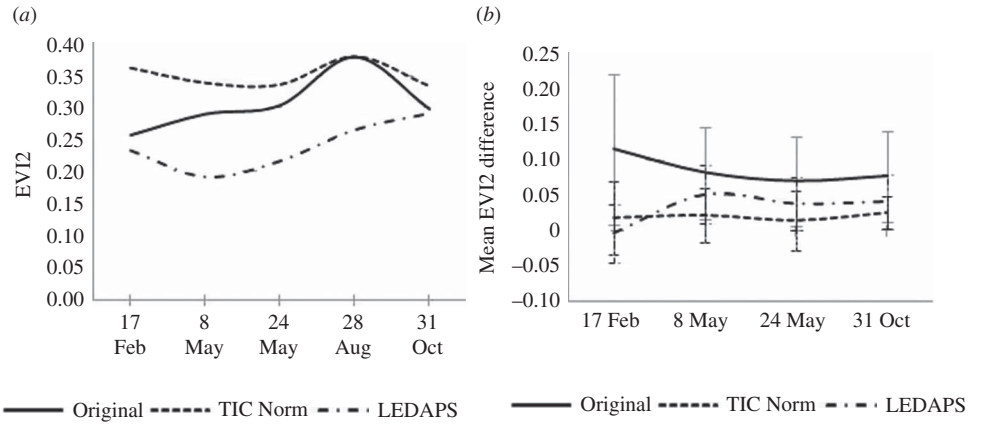

Figure 8. (*a*) Line graph showing overall EVI2 means for Wicklow Mountains ETM+ subset images based on original, TIC subset normalization, and LEDAPS pre-processing. (*b*) Graph of mean difference between master and slave images for part (*a*) (and order as for part (*a*)) data sets. The ends of the error bars represent +1 or –1 standard deviation from the mean.

data (O Connell, Connolly, and Holden in review-a). Further investigations are needed to establish the cause of this trend in the absolute corrected EVI2 data over peatland, but it is likely that the vegetation dynamics of Heather (*Calluna*) and *Sphagnum* species in such habitats is different to that of other vegetation types with a higher chlorophyll content (i.e. woodlands and natural grassland).

An analysis of the variability in radiometric characteristics between master and slave images for the three data sets shows a far more gradual trend across the temporal scale of the data base for the TIC-subset-normalized data (Figure 8(*b*)). The difference statistics were calculated from pixel-to-pixel subtraction, with mean values representing the complete study area outlined in Figure 1. Again, the TIC-subset-normalized data indicated a more gradual trend when compared to the original data, with mean difference between master and slave not exceeding 0.03 EVI2. The trend in the TIC subset data, unlike the Original data, did not show a significant increase in difference values for the February and October images. This illustrates the robustness of the TIC subset normalization process, as increasing the temporal distance between master and slave images does not reduce the effectiveness of the normalization procedure. The LEDAPS data showed an irregular pattern, which oscillated between 0 and 0.05 EVI2. This demonstrates the radiometric inconsistency associated with *in situ* absolute correction, and the effect these inconsistencies may have on a change detection study (Song et al. 2001; Schroeder et al. 2006).

Image histograms (Figure 9) for master, slave, and TIC-normalized data showed a clear increase in radiometric correlation due to the TIC subset normalization process. The 17 February slave image showed a notable deviation in its histogram profile when plotted against the 28 August master image (Figure 9(*a*)). The effectiveness of the TIC subset normalization process was evident by the re-scaling of the slave data (TIC Norm) to a profile similar to that of the master image (Figure 9(*a*)). Cumulative distribution (CD) curves were also calculated for master, slave, and TIC-subset-normalized data by first calculating the frequency proportions at all bin values in the histogram. Cumulative proportions were then calculated by continuously adding proportion values from the previous bin number. Cumulative proportions were then subtracted from each image, with the maximum value

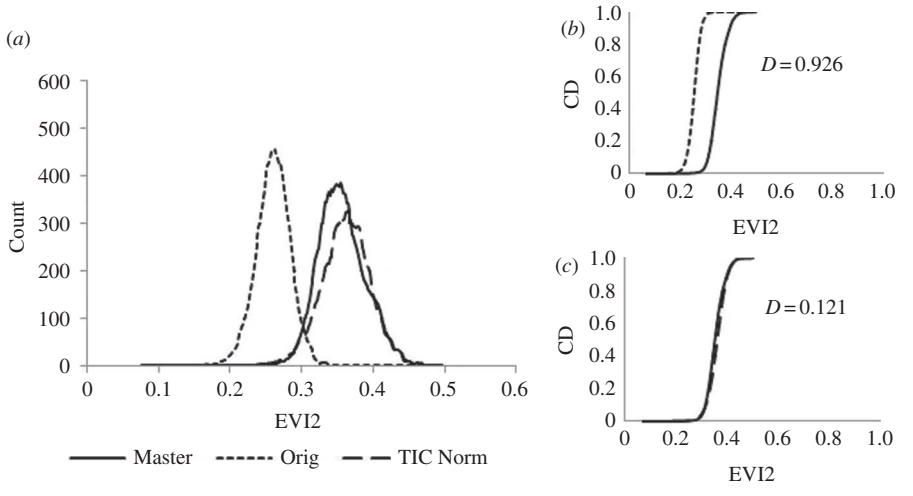

Figure 9. EVI2 image histograms (*a*) and cumulative distribution (CD) curves (*b*) and (*c*), with accompanying *D* values, for 17 February 2001 slave image (Orig), 17 February 2001 normalized image (TIC Norm), and 28 August master image (Master).

(D in Figures 9(*b*) and (*c*)) representing the maximum difference between the two images in question. The effect of the TIC subset normalization can be seen by the significantly increased correlation of the master versus normalized data (Figure 9(*c*)) when compared to the master versus slave data (Figure 9(*b*)). This increased correlation was quantified by an 86.93% decrease in the maximum difference due to the TIC subset normalization process.

4. Conclusions

This study has shown that radiometric normalization is a critical stage in a change detection study. If ignored, variations in atmospheric conditions, sun's elevation, and sensor view angle reduce the accuracy of any change detection analysis due to variations in spectral response between images. Previous studies have demonstrated the value of pseudo-invariant features in the normalization of multi-temporal multi-spectral data. This study has demonstrated the value of a revised TIC subset normalization method for the extraction and dissemination of invariant clusters from satellite imagery. The use of density slices and regional growth functions to locate and delineate urban and water pixels has resulted in a spectrally homogeneous scatter plot in which spatial statistics can be readily applied to accurately define cluster centres and resulting regression function coefficients. This focused approach has advantages over other more holistic methods of invariant cluster normalization, especially in landscapes with a low distribution of radiometrically stable targets.

Validation results indicated a high correlation between the TIC-subset-normalized and LEDAPS-corrected imagery. The stable trends in mean EVI2, both in terms of overall mean and land-use-specific means, indicated the viability of the TIC subset normalization procedure for the radiometric correction of a multi-temporal data base of multi-spectral imagery. The effect of increased temporal distance between master and slave images had a minimal effect on correlation with the equivalent absolute corrected data, demonstrating that the TIC subset normalization procedure was ideal for its application when dealing with a data

base of high temporal resolution. Statistical analysis on the correlation between master, slave and normalized slave data showed an 86.93% reduction in the maximum difference in CD curves between master and slave data due to the TIC subset normalization process.

The revised TIC subset normalization method developed in this study is semi-automated and easy to apply. The normalized images can be readily utilized in a change detection system for further analysis. The normalization procedure is especially suitable for studying landscapes with a low density of spectrally stable targets.

Acknowledgements

The authors wish to thank the Environmental Protection Agency of Ireland (EPA) for their financial support under the STRIVE fellowship. The authors also wish to thank the US Geological Survey for providing access to the ETM+ data, as well as the NPWS for supplying habitat maps of the Wicklow Mountains National Park.

References

Bragg, O. M., and J. H. Tallis. 2001. "The Sensitivity of Peat-Covered Upland Landscapes." *Catena* 42: 345–60.

Brennan, P., and J. Curtin. 2008. *The Climate Change Challenge. Strategic Issues, Options and Implications for Ireland*. Dublin: Institute of International and European Affairs.

Chen, X., L. Vierling, and D. Deering. 2005. "A Simple and Effective Radiometric Correction Method to Improve Landscape Change Detection across Sensors and across Time." *Remote Sensing of Environment* 98: 63–79.

Civco, D. 1989. "Topographic Normalization of Landsat Thematic Mapper Digital Imagery." *Photogrammetric Engineering and Remote Sensing* 55: 1303–9.

Connolly, J., N. M. Holden, J. Connolly, J. W. Seaquist, and S. M. Ward. 2011. "Detecting Recent Disturbance on Montane Blanket Bogs in the Wicklow Mountains, Ireland Using the MODIS Enhanced Vegetation Index." *International Journal of Remote Sensing* 32: 2377–93.

Connolly, J., N. M. Holden, and S. M. Ward. 2006. *Detecting Vegetation Change with Remote Sensing: An Evaluation of Threshold Limits for Blanket Bog*. Dublin: University College Dublin.

Coppin, P., I. Jonckheere, K. Nackaerts, and B. Muys. 2004. "Digital Change Detection Methods in Ecosystem Monitoring: A Review." *International Journal of Remote Sensing* 25: 32.

CSO. 2006. *2006 Census of Population – Classified by Area*, Volume 1. Dublin: Central Statistics Office.

Dabrowska-Zielinska, K., M. Gruszczynska, S. Lewinski, A. Hoscilo, and J. Bojanowski. 2009. "Application of Remote and In Situ Information to the Management of Wetlands in Poland." *Journal of Environmental Management* 90: 2261–9.

Du, Y., P. M. Teillet, and J. Cihlar. 2002. "Radiometric Normalization of Multitemporal High-Resolution Satellite Images with Quality Control for Land Cover Change Detection." *Remote Sensing of Environment* 82: 123–34.

Eaton, J., N. McGoff, K. Byrne, P. Leahy, and G. Kiely. 2008. "Land Cover Change and Soil Organic Carbon Stocks in the Republic of Ireland 1851–2000." *Climatic Change* 91: 317–34.

Eckhardt, D., J. Verdin, and G. Lyford. 1990. "Automated Update of an Irrigated Lands GIS Using SPOT HRV Imagery." *Photogrammetric Engineering and Remote Sensing (USA)* 56: 1515–22.

ESRI. 2010. *ArcGIS Desktop: Release 9.3*. Redlands, CA: Environmental Systems Research Institute.

Fossitt, J. 2000. *A Guide to Habitats in Ireland*. Dublin: Heritage Council/Chomhairle Oidhreachta.

Gao, Y., and W. Zhang. 2009. "A Simple Empirical Topographic Correction Method for ETM+ Imagery." *International Journal of Remote Sensing* 30: 2259–75.

Hajj, M. El., A. Begue, B. Lafrance, O. Hagolle, and M. Rumeau. 2008. "Relative Radiometric Normalization and Atmospheric Correction of a SPOT 5 Time Series." *Sensors* 8: 2774–91.

Hassan, Q., and P. Charles. 2010. "Spatial Enhancement of MODIS-Based Images of Leaf Area Index: Application to the Boreal Forest Region of Northern Alberta, Canada." *Remote Sensing* 2: 278–89.

Huete, A., K. Didan, T. Miura, E. Rodriguez, X. Gao, and L. Ferreira. 2002. "Overview of the Radiometric and Biophysical Performance of the MODIS Vegetation Indices." *Remote Sensing of Environment* 83: 195–213.

Huete, A., H. Liu, K. Batchily, and W. Van Leeuwen. 1997. "Comparison of Vegetation Indices over a Global Set of TM Images for EOS-MODIS." *Remote Sensing of Environment* 59: 440–51.
Janzen, D. T., A. L. Fredeen, and R. D. Wheate. 2006. "Radiometric Correction Techniques and Accuracy Assessment for Landsat TM Data in Remote Forested Regions." *Canadian Journal of Remote Sensing* 32: 10.
Jiang, Z., A. Huete, K. Didan, and T. Miura. 2008. "Development of a Two-Band Enhanced Vegetation Index without a Blue Band." *Remote Sensing of Environment* 112: 3833–45.
Jin, S., and S. A. Sader. 2005. "Comparison of Time Series Tasseled Cap Wetness and the Normalized Difference Moisture Index in Detecting Forest Disturbances." *Remote Sensing of Environment* 94: 364–72.
Justice, C., J. Townshend, E. Vermote, E. Masuoka, R. Wolfe, N. Saleous, D. Roy, and J. Morisette. 2002. "An Overview of MODIS Land Data Processing and Product Status." *Remote Sensing of Environment* 83: 3–15.
Kyoto Protocol. 1997. *United Nations Framework Convention on Climate Change*. New York: United Nations.
Levy, R. C., L. A. Remer, and O. Dubovik. 2007. "Global Aerosol Optical Properties and Application to Moderate Resolution Imaging Spectroradiometer Aerosol Retrieval over Land." *Journal of Geophysical Research* 112: D13210.
Lillesand, T. M., R. W. Kiefer, and J. W. Chipman. 2004. *Remote Sensing and Image Interpretation*. Chichester: Wiley.
Masek, J., E. Vermote, N. Saleous, R. Wolfe, F. Hall, K. Huemmrich, F. Gao, J. Kutler, and T. Lim. 2006. "A Landsat Surface Reflectance Dataset for North America, 1990–2000." *IEEE Geoscience and Remote Sensing Letters* 3: 68–72.
McGovern, E. A., N. M. Holden, S. M. Ward, and J. F. Collins. 2002. "The Radiometric Normalization of Multitemporal Thematic Mapper Imagery of the Midlands of Ireland – A Case Study." *International Journal of Remote Sensing* 23: 751–66.
McMorrow, M. J. M., M. E. J. Cutler, M. G. Evans, and A. Al-Roichdi. 2004. "Hyperspectral Indices for Characterizing Upland Peat Composition." *International Journal of Remote Sensing* 25: 313–25.
NASA. 1998. *Landsat 7 Science Data Users Handbook*. Accessed July 23, 2008. http://landsathandbook.gsfc.nasa.gov/handbook/handbook_toc.html.
Nichol, J., L. Hang, and W. Sing. 2006. "Empirical Correction of Low Sun Angle Images in Steeply Sloping Terrain: A Slope-Matching Technique." *International Journal of Remote Sensing* 27: 629–35.
NPWS (National Parks and Wildlife Service) 2007. *Vegetation and Habitat Survey of Wicklow Upland SAC*, 1–35. Malvern: National Parks and Wildlife Service.
O Connell, J. 2012. *Large-Scale Monitoring of Disturbance to Irish Peatlands Using Satellite Remote Sensing*. Dublin: University College Dublin.
O Connell, J., J. Connolly, and N. M. Holden. In review-a. "Can Leaf Area Index Estimated from Satellite Imagery Be Used as an Indicator of Disturbance of Irish Peatlands?" *Irish Geography*.
O Connell, J., J. Connolly, and N. M. Holden. In review-b. "Multispectral, Multiplatform Detection of Peatland Vegetation Change Indicative of Disturbance." *Journal of Applied Remote Sensing*.
Ozesmi, S. L., and M. E. Bauer. 2002. "Satellite Remote Sensing of Wetlands." *Wetlands Ecology and Management* 10: 22.
Paolini, L., F. Grings, J. Sobrion, J. Jimenez Munoz, and H. Karszenbaum. 2006. "Radiometric Correction Effects in Landsat Multi-Date/Multi-Sensor Change Detection Studies." *International Journal of Remote Sensing* 27: 685–704.
Qi, J., A. Chehbouni, A. Huete, Y. Kerr, and S. Sorooshian. 1994. "A Modified Soil Adjusted Vegetation Index." *Remote Sensing of Environment* 48: 119–26.
Riaño, D., E. Chuvieco, J. Salas, and I. Aguado. 2003. "Assessment of Different Topographic Corrections in Landsat-TM Data for Mapping Vegetation Types." *IEEE Transactions on Geoscience and Remote Sensing* 41: 1056–61.
Richards, J. A., and X. Jia. 2006. *Remote Sensing Digital Image Analysis: An Introduction*. New York: Springer.
Rocha, A., and G. Shaver. 2009. "Advantages of a Two Band EVI Calculated from Solar and Photosynthetically Active Radiation Fluxes." *Agricultural and Forest Meteorology* 149: 1560–3.
Rondeaux, G., M. Steven, and F. Baret. 1996. "Optimization of Soil-Adjusted Vegetation Indices." *Remote Sensing of Environment* 55: 95–107.

Schroeder, T., W. Cohen, C. Song, M. Canty, and Z. Yang. 2006. "Radiometric Correction of Multi-Temporal Landsat Data for Characterization of Early Successional Forest Patterns in Western Oregon." *Remote Sensing of Environment* 103: 16–26.

Sellers, P. 1985. "Canopy Reflectance, Photosynthesis and Transpiration." *International Journal of Remote Sensing* 6: 1335–72.

Song, C., C. E. Woodcock, K. C. Seto, M. P. Lenney, and S. A. Macomber. 2001. "Classification and Change Detection Using Landsat TM Data: When and How to Correct Atmospheric Effects?" *Remote Sensing of Environment* 75: 15.

Tallis, J. H.. 1998. "Growth and Degradation of British and Irish Blanket Mires." *Environmental Reviews* 6: 81–122.

Teillet, P. M., K. Staenz, and D. J. William. 1997. "Effects of Spectral, Spatial, and Radiometric Characteristics on Remote Sensing Vegetation Indices of Forested Regions." *Remote Sensing of Environment* 61: 139–49.

Tomlinson, R. W. 2005. "Soil Carbon Stocks and Changes in the Republic of Ireland." *Journal of Environmental Management* 76: 77–93.

USGS. 2010. *USGS Global Visualization Viewer (GloVis)*. 8.6 ed. Accessed March 10, 2010. www.glovis.usgs.gov.

Vermote, E. F., D. Tanre, J. L. Deuze, M. Herman, and J. J. Morcette. 1997. "Second Simulation of the Satellite Signal in the Solar Spectrum, 6s: An Overview." *IEEE Transactions on Geoscience and Remote Sensing* 35: 675–86.

Vicente-Serrano, S. M., F. Perez-Cabello, and T. Lasanta. 2008. "Assessment of Radiometric Correction Techniques in Analyzing Vegetation Variability and Change Using Time Series of Landsat Images." *Remote Sensing of Environment* 112: 3916–34.

Wilson, E. H., and S. A. Sader. 2002. "Detection of Forest Harvest Type Using Multiple Dates of Landsat TM Imagery. *Remote Sensing of Environment* 80: 385–96.

Yu, Z., J. Loisel, D. Brosseau, D. Beilman, and S. Hunt. 2010. "Global Peatland Dynamics since the Last Glacial Maximum." *Geophysical Research Letters* 37: 1–5.